2022

Biofabrication of magnetic nanoparticles and their use as carriers for pectinase and xylanase

Shady S. Hassan

Brendan Duffy

Gwilym A. Williams

See next page for additional authors

Funder: Technological University Dublin

Authors
Shady S. Hassan, Brendan Duffy, Gwilym A. Williams, and Amit Jaiswal

OpenNano 6 (2022) 100034

Contents lists available at ScienceDirect

OpenNano

journal homepage: www.elsevier.com/locate/onano

Biofabrication of magnetic nanoparticles and their use as carriers for pectinase and xylanase

Shady S. Hassan [a,b,c], Brendan Duffy [d], Gwilym A. Williams [c], Amit K. Jaiswal [a,b,*]

[a] School of Food Science and Environmental Health, Technological University Dublin, City Campus, Central Quad, Grangegorman, Dublin, D07 ADY7, Ireland
[b] Environmental Sustainability and Health Institute, Technological University Dublin, City Campus, Grangegorman, Dublin D07 H6K8, Ireland
[c] School of Biological Sciences and Health Sciences, Technological University Dublin - City Campus, Central Quad, Grangegorman, Dublin, D07 ADY7, Ireland
[d] Centre for Research in Engineering and Surface Technology (CREST), FOCAS Institute, Technological University Dublin - City Campus, Kevin Street, Dublin D08 NF82, Ireland

ARTICLE INFO

Keywords:
Magnetite nanoparticles
A. flavus
M. hiemalis
Pectinase
Xylanase
Immobilization

ABSTRACT

In this study, superparamagnetic iron oxide nanoparticles (MNPs) were synthesized via exposure of fungal cell filtrate from *Aspergillus flavus* to aqueous iron ions. The extracellular synthesis of MNPs was monitored by UV–Vis spectrophotometry and showed an absorption peak at 310 nm. The morphology of MNPs was found to be flake-like, as confirmed by Field Emission Scanning Electron Microscopy (FESEM), while the average crystallite size was ~16 nm, as determined by X-ray diffraction (XRD). Energy dispersive X-ray (EDX) analysis was performed to confirm the presence of elemental Fe in the sample. Pectinase and xylanase were covalently immobilized on MNPs with efficiencies of ~84% and 77%, respectively. Compared to the free enzymes, the immobilized enzymes were found to exhibit enhanced tolerance to variation of pH and temperature and demonstrated improved storage stability. Furthermore, the residual activity of the immobilized enzymes was about 56% for pectinase and 52% for xylanase, after four and three consecutive use cycles, respectively.

1. Introduction

Immobilized enzymes are of prime importance for some commercial processes, with the key advantage of biocatalyst recycling often being complemented by higher operational stability, and a lower risk of product contamination with enzyme [1]. However, depending on the immobilization method employed, such advantages can be offset by additional process costs, up to 25 times that of the free enzyme [2]. Therefore, there is considerable interest in exploring the potential of nanoparticles as a low-cost platform for enzyme immobilization.

Nanoparticles (1–100 nm in size) have gained prominence in the modern era, as they constitute the building blocks for tailored nanocomposites that can be exploited in a wide range of novel applications. In 2017, nanocomposites had a market value amounting to nearly $2 billion (USD) worldwide, and this is projected to increase to over $7 billion (USD) by 2022 at a compounded annual growth rate (CAGR) of 29.5% during the forecast period of 2017 to 2022 [3]. Driven by global environmental challenges, the industrial

* Corresponding author.
E-mail address: amit.jaiswal@TUDublin.ie (A.K. Jaiswal).

https://doi.org/10.1016/j.onano.2021.100034
Received 27 May 2021; Received in revised form 25 November 2021; Accepted 6 December 2021
Available online 7 December 2021

revolution in the 21st century is likely to be based on renewable biological resources. In this regard, bio-nanotechnology has emerged as a promising field of research that builds on nanotechnology and biotechnology.

Of all the nanoparticles studied so far, magnetic nanoparticles (MNPs) are of interest for enzyme immobilization owing to their ease of separation in a reaction and chemical inertness [4]. Moreover, the advent of microbially-produced MNPs has created a paradigm shift in enzyme immobilization technology, providing favorable process economics and offering the additional advantage of mild reaction conditions for their production [5,6]. Therefore, microbial production of nanoparticles is rapidly becoming a favored approach in this field [7]. In this respect, filamentous fungi have been used chiefly in the synthesis of metal nanoparticles due to their wide array of extracellular enzymes and high metal tolerance [8].

A review of the literature in this field indicates a degree of heterogeneity in terms of fungal species being investigated in the biosynthesis of magnetic nanoparticles (e.g. *Fusarium oxysporum* [9], *Fusarium incarnatum* [10], *Trichoderma asperellum* [10], *Phialemoniopsis ocularis* [10], *Verticillium sp*. [9], *Aspergillus niger* [11,12], *Aspergillus oryzae* [13], and *Aspergillus japonicus* [14]). However, to the best knowledge of the authors, no work in this field has yet been reported using *Aspergillus flavus* for synthesis of MNPs. Therefore, the present study investigates the use of *A. flavus* to produce MNPs and explores their application in enzyme immobilization. To date, MNPs have been extensively studied for immobilization of pectinase [15–20] and xylanase [21–29] for easy separation and reuse. Therefore, pectinase and xylanase were used as model enzymes in this study for immobilization on MNPs. Hence, the novelty of this study lies in the utilization of *A. flavus* to produce MNPs and its subsequent application in pectinase and xylanase immobilization (as model enzymes).

2. Materials and methods

2.1. Chemicals

Pectinase (912 U/ml) and xylanase (455 U/ml) were produced from *Mucor hiemalis* AB1 (GenBank accession number: JQ912672.1) in our laboratory [30]. Enzyme activity was determined by the dinitrosalicylic acid (DNS) method of Miller [31] using pectin (citrus peel) or xylan (beechwood) as standard. Unless stated, all other chemicals including pectin, xylan, ferric chloride, ferrous chloride, glutaraldehyde, Sabouraud dextrose broth and agar were purchased from Sigma Aldrich (Ireland), and were of analytical grade.

2.2. Isolation of Aspergillus sp. SR2

The fungus, *Aspergillus sp*. SR2, was isolated from spoiled strawberry (variety: Rociera) in a previous study [30]. In the latter, the isolated strain was preliminarily identified to the genus level based on macroscopic morphology and microscopic features (results not shown). The isolate was stored at 4 °C on SDA slopes (Sabouraud dextrose agar; 40 g/l dextrose, 10 g/l mycological peptone, and 15 g/l agar) for further study.

2.3. Molecular Identification of Aspergillus sp. SR2

Initially, the genomic DNA was extracted using PrepMan® Ultra Sample Preparation Reagent following the instructions of the manufacturer (Thermo Fisher Scientific Inc., Waltham, MA, USA). The internal transcribed spacer (ITS) regions of ribosomal DNA were then amplified using universal primers: ITS1 (forward, 5′-CTTGGTCATTTAGAGGAAGTAA-3′), ITS4 (reverse, 5′-TCCTCCGCTTATTGATATGC-3′), and MyTaq™ DNA Polymerase Kit (Bioline, London, UK) [32]. The PCR products were then purified using ExoSAP-IT® (Thermo Fisher Scientific Inc., Waltham, MA, USA), followed by Sanger sequencing (LGC Genomics GmbH, Berlin, Germany). Finally, the resulting nucleotide sequences were processed with the software Chromas (V 2.6.6, Technelysium, Brisbane, Australia) and compared using a Basic Local Alignment Search Tool (BLAST) with sequences deposited in the National Center for Biotechnology Information (NCBI) Nucleotide database (blast.ncbi.nlm.nih.gov).

2.4. Biosynthesis of magnetic nanoparticles

The protocol reported by Mahanty et al. [10] was followed with minor modifications. Briefly, the fungal isolate was grown in potato dextrose broth (PDB; 250 ml Erlenmeyer flask with a working volume of 20%) with orbital shaking (120 rpm, 25 °C). After 14 days of incubation, the culture fluid was separated from fungal biomass by filtration through Whatman filter paper no. 1, followed by centrifugation at 5000 rpm for 5 min. The final filtrate (10 ml) was later utilized for the reduction of iron salts in aqueous solution (5 ml) consisting of 2 mM Iron (III) and 1 mM Iron (II) chloride mixture (2:1). The reaction mixture was agitated for 5 min at room temperature, and color changes were observed and considered as a positive result for the development of MNPs. Next, the MNPs were collected by centrifugation at 12,000 rpm for 15 min and washed three times with deionized water. Finally, MNPs were obtained after magnetic separation and immediately re-dispersed in deionized water and sonicated (Fisher Scientific TI-H-10 Ultrasonic bath, output 750 W) for 1 hour to separate the MNPs into individual particles. The culture filtrate (without iron salts) and salt solution (without culture filtrate) were considered as positive and negative controls, respectively.

2.5. Characterization of MNPs

The absorption spectra of MNPs were measured in the wavelength range from 200 to 800 nm using a UV-1800 UV–VIS

spectrophotometer (Shimadzu Scientific Instruments, Columbia, USA). Powder X-Ray diffraction (XRD) analysis was carried out with a Siemens D500 diffractometer (Berlin, Germany) to study the crystal structure of the MNPs. XRD data was analyzed using the Origin Pro 8 software (Trial version, Microcal Software Inc., USA), and the average crystallite size of the MNPs was estimated using the Scherrer equation [33]. The morphology (particle shape) of the MNPs were observed using a Hitachi SU 70 (Hitachi High Technologies, Japan) field emission scanning electron microscope (FESEM). The FESEM system was equipped with an X-Max silicon drift detector (Oxford Instruments, UK) for energy dispersive X-ray (EDX) analysis to confirm the presence of iron in the particles, as well as to characterize the other elementary composition of the particles.

2.6. Immobilization of biocatalysts on MNPs

A two-step procedure was followed to immobilize pectinase and xylanase on MNPs adopted from previously reported methods, with minor modifications [34, 35]. The first step was the activation of the MNPs (50 mg) by suspension in glutaraldehyde solution (1.0 M, 5 ml) for 2 h at 37 °C under constant mechanical stirring. The next step involved the covalent binding of the glutaraldehyde-activated MNPs (50 mg, MNPs@GLU) to pectinase or xylanase (1 mL) by incubating the suspension for 24 h at 37 °C under constant mechanical stirring. Finally, enzyme-functionalized MNPs (MNPs@GLU-ENZ) were obtained after magnetic separation and washed with deionized water to remove loosely or unbound proteins. The immobilization yield, and activity recovery of immobilized pectinase or xylanase, were calculated as follows:

$$\text{Immobilization yield } (\%) = \frac{(C_{init} - C_{fin})}{C_{init}} \text{ x } 100$$

where C_{fin} is the amount of protein in the supernatant (enzyme solution) after magnetic separation and C_{init} is the total protein available for immobilization, as determined by the Bradford assay [36, 28, 37]

$$\text{Activity recovery } (\%) = \frac{A_{immob}}{A_{init}} \text{ x } 100$$

where A_{immob} is the immobilized enzyme activity and A_{init} is the initial (free) enzyme activity as determined by the Miller DNS assay [38].

2.7. Evaluation of the nano-immobilized enzymes (MNPs@GLU-ENZ)

The optimum reaction pH of MNPs@GLU-ENZ was determined over the range between 2.0 and 11.0 using glycine-HCl buffer (0.1 M, pH 2.0), citrate buffer (0.1 M, pH 3.0–6.0), phosphate buffer (0.1 M, pH 7–8) and glycine-NaOH buffer (0.1 M, pH 9–11), while the optimum temperature was investigated between 20 °C and 80 °C [30]. To evaluate the storage stability, MNPs@GLU-ENZ were held for 30 days at 4 °C [39]. For a reusability assessment, MNPs@GLU-ENZ were recovered with magnetic separation after each cycle of use, washed with deionized water, and then a new cycle was run under the same conditions for a total of 6 cycles [19]. The enzyme activity in the first cycle was assigned a relative activity of 100%, and relative activity was calculated for the successive cycles. All experiments were performed in triplicate.

3. Results and discussion

3.1. Molecular Identification of Aspergillus sp. SR2

Aspergillus sp. isolate used in the current study was previously isolated in our lab from spoiled strawberry (variety: Rociera). Molecular identification of fungal isolate was carried out by analyzing the sequences of the ITS region of ribosomal DNA (ITS1–5.8S-ITS2) and pairwise sequence alignment using the BLAST algorithm. The resultant nucleotide sequence in this study (Table 1) matched 100% with the published sequence of *Aspergillus flavus* (Accession No. MN238861.1) available in GenBank. The aforementioned taxon

Table 1
Nucleotide sequences of *Aspergillus flavus* SR2.

1	GAGGAAGTAA	AAGTCGTAAC	AAGGTTTCCG	TAGGTGAACC	TGCGGAAGGA	TCATTACCGA
61	GTGTAGGGTT	CCTAGCGAGC	CCAACCTCCC	ACCCGTGTTT	ACTGTACCTT	AGTTGCTTCG
121	GCGGGCCCGC	CATTCATGGC	CGCCGGGGGC	TCTCAGCCCC	GGGCCCGCGC	CCGCCGGAGA
181	CACCACGAAC	TCTGTCTGAT	CTAGTGAAGT	CTGAGTTGAT	TGTATCGCAA	TCAGTTAAAA
241	CTTTCAACAA	TGGATCTCTT	GGTTCCGGCA	TCGATGAAGA	ACGCAGCGAA	ATGCGATAAC
301	TAGTGTGAAT	TGCAGAATTC	CGTGAATCAT	CGAGTCTTTG	AACGCACATT	GCGCCCCCTG
361	GTATTCCGGG	GGGCATGCCT	GTCCGAGCGT	CATTGCTGCC	CATCAAGCAC	GGCTTGTGTG
421	TTGGGTCGTC	GTCCCCTCTC	CGGGGGGGAC	GGGCCCCAAA	GGCAGCGGCG	GCACCGCGTC
481	CGATCCTCGA	GCGTATGGGG	CTTTGTCACC	CGCTCTGTAG	GCCCGGCCGG	CGCTTGCCGA
541	ACGCAAATCA	ATCTTTTTCC	AGGTTGACCT	CGGATCAGGT	AGGGATACCC	GCTGAACTTA
601	AGCATAT					

is one of the most common fungi that are found on strawberry fruit, as previously reported [40].

3.2. Biosynthesis of magnetic nanoparticles

Biosynthesis of MNPs using culture filtrate of *A. flavus* was initiated rapidly after treatment with iron salts, which was visualized by observing the change in color of the reaction mixture from yellow to black (Fig. 1), while no visible color change was observed for either positive and negative controls.

Few studies to date have investigated the capability of fungi for the production of magnetic nanoparticles, and most of these studies have focused on *Aspergillus* species, such as *Aspergillus niger* [11,12], *Aspergillus oryzae* [13], and *Aspergillus japonicus* [14]. In the aforementioned studies on *Aspergillus* species, different iron salts were utilized, such as potassium ferricyanide and potassium ferrocyanide salts solution [14], ferrous sulfate and ferric chloride salts solution [11,12], and ferric chloride solution [13]. Thus, our study brings a novel approach for the biosynthesis of MNPs by *Aspergillus* species where filtrate of *A. flavus* reduced the ferrous chloride and ferric chloride salts solution. According to the available literature, the exact mechanism for the biosynthesis of metal oxide NPs by fungi has not yet been elucidated. However, the biomineralization process could have occurred via reducing iron metal ions by extracellular redox enzymes from *A. flavus* [41].

3.3. Characterization of MNPs

The detailed characterization of the mycosynthesized MNPs was performed using UV–vis spectrophotometry, Field Emission Scanning Electron Microscopy (FESEM), Energy dispersive X-ray (EDX) and X-ray diffraction (XRD). The UV–vis absorption spectra (Fig. 2) shows a characteristic absorption band at 310 nm, confirming the formation of MNPs [42]. Furthermore, the EDX spectrum and elemental mapping as shown in Fig. 3 detected the presence of Fe and O. The Fe and O element mapping further confirmed that the two constituent elements were well-distributed over the sample. However, the spectrum also revealed small traces of impurities which presumably originated from the iron salts and the *A. flavus* filtrate used for the synthesis of MNPs [43].

The SEM images (Fig. 4) of MNPs show clusters of flake-like morphology. Similar morphology was also observed by Chatterjee et al. [12], who studied MNPs produced by *Aspergillus niger* BSC-1. Bharde et al. [9] also reported the biosynthesis of irregular MNPs using *Fusarium oxysporum*. The observed flake-like morphology could be due to the binding activity of biomolecules of *A. flavus* on the growing particles of Fe_3O_4 [44]. Additionally, there is a possibility of imperfect drying of the MNPs using the vacuum drying technique (GeneVac EZ-2 Plus evaporator, Genevac Ltd, Ipswich, UK). Thus, one possible solution would be to use vacuum freeze-drying of liquid nanoparticle dispersions to produce a lyophilized MNP powder which may minimize aggregate formation; in turn, this could lead to a modified particle size distribution. Above all, MNPs tends to agglomerate into larger clusters in order to reduce their surface energy [45], in a phenomenon known as Ostwald ripening [46]. Thus, XRD was used to estimate the average crystallite size of individual (primary) particles .

Fig. 5 shows the XRD patterns for MNPs with six characteristic peaks for Fe_3O_4 marked by their indices (220), (311), (400), (422), (511), and (440). The results of phase analysis agree with the reference magnetite Fe_3O_4 pattern from the Joint Committee on Powder Diffraction Standards (JCPDS card number 19–0629), and published literature [47,48]. Due to the size of the small crystallites, only

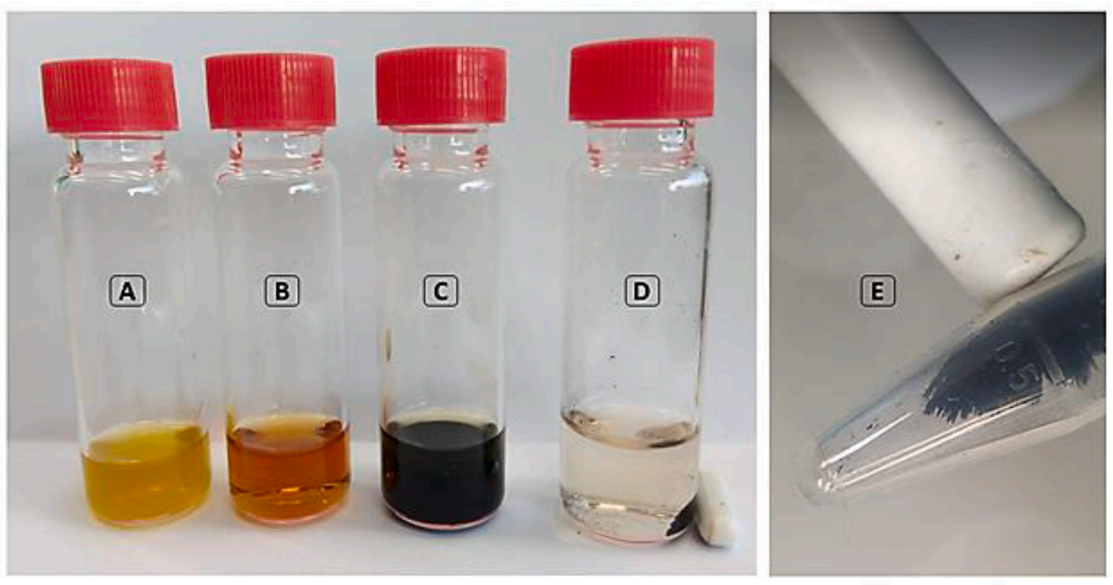

Fig. 1. The culture filtrate of *A. flavus* (A), iron salts solution (B), black coloration due to mixing of solutions $A + B$ for 5 min (C), separation of MNPs from reaction mixture using an external magnet (D), and the magnetic behavior of dried MNPs in the presence of a magnet (E).

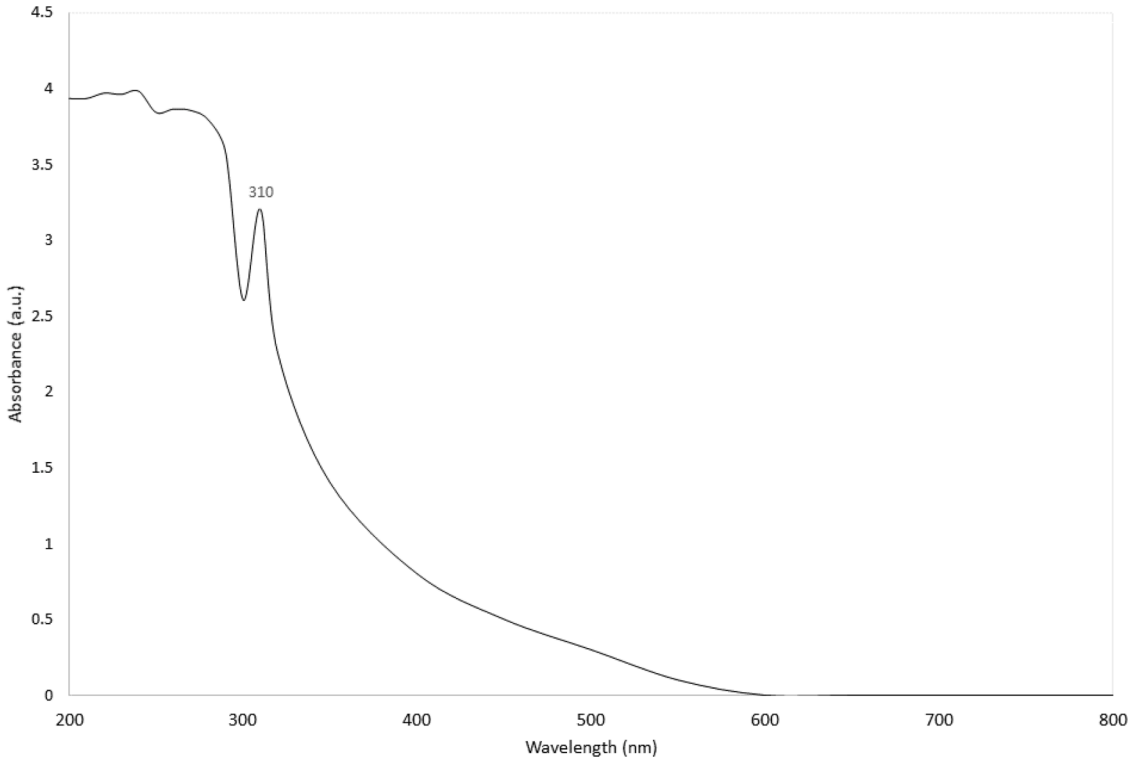

Fig. 2. UV–vis spectrum of MNPs.

one major peak at 35.3° corresponding to the (311) plane was detected, while other peaks for magnetite were less distinctive [49]. Therefore, the full width at half maximum (FWHM) of the (311) peak was used to calculate the crystallite size. The average crystallite size of the MNPs was ~16 nm, as estimated by the Scherrer equation. Comparisons with the literature revealed that MNPs derived from fungi were in the size range of 10 to 40 nm [12,50]. MNPs smaller than the critical size of 20 nm are known to be superparamagnetic, with a high magnetization value [51]. The aforementioned superparamagnetic iron oxide nanoparticles are of industrial interest due to their low toxicity, and good biocompatibility [52]. Thus, superparamagnetic iron oxide nanoparticles are versatile carriers for realizing enzyme immobilization that facilitates catalyst separation.

3.4. Immobilization of biocatalysts on MNPs

Direct immobilization of pectinase and xylanase on MNPs is not effective because of surface oxidation and rejection [53]. Thus, MNPs were subjected to glutaraldehyde treatment for the activation of MNPs which facilitates the formation of the Schiff base linkage between the aldehyde group of glutaraldehyde and the terminal amino group of enzymes [54]. Finally, the activated MNPs (MNPs@GLU) were treated with pectinase or xylanase individually to produce enzyme-functionalized MNPs (MNPs@GLU-ENZ). Immobilization yields of pectinase- and xylanase-functionalized MNPs were about 84% and 77%, respectively. For pectinase, the immobilization yield of this work (84%) was much higher than that (51%) previously reported by Mosafa et al. [19] using silica-coated magnetite nanoparticles via a sol–gel approach. The use of the latter may result in composite particles with an ill-defined structure due to the formation of aggregates [61], and this may affect the enzyme immobilization yield. Another reason could be that these enzymes are of different origin, and therefore are most likely to be structurally different. It follows that the immobilization yield would most probably be different. This may also be the reason why a previous study reported a higher yield (92%) of xylanase from *Bacillus sp.* NG-27 when immobilized on glutaraldehyde-activated magnetic nanoparticles [28]. It is known that a wide number of factors can affect the immobilization yield using this method, including surface area activation, stirring speed, enzyme load, MNP proportion, and enzyme-MNP coupling time [54].

The recovery of enzyme activity remaining in immobilized pectinase and xylanase were about 74% and 68%, respectively. For pectinase, the activity recovery of this work (74%) was much lower than that (92%) previously reported by Nadar and Rathod [20] using amino-activated magnetite nanoparticles, and the 85% activity recovery reported by Muley et al. [55] using glutaraldehyde-activated magnetic nanoparticles. Also, the latter study reported higher activity recovery of xylanase (76%) compared to the activity recovery of xylanase (68%) in the present work. However, Perwez et al. [56] reported similar xylanase activity (69%) when immobilized on 3-aminopropyl triethoxysilane-activated magnetic nanoparticles. The use of 3-Aminopropyl triethoxysilane (APTES) for particle functionalization prior to glutaraldehyde cross-linking [20, 55] has previously proved to be a viable approach to achieve improved enzyme immobilization. However, an integral part of this work was the adoption of green chemistry immobilization

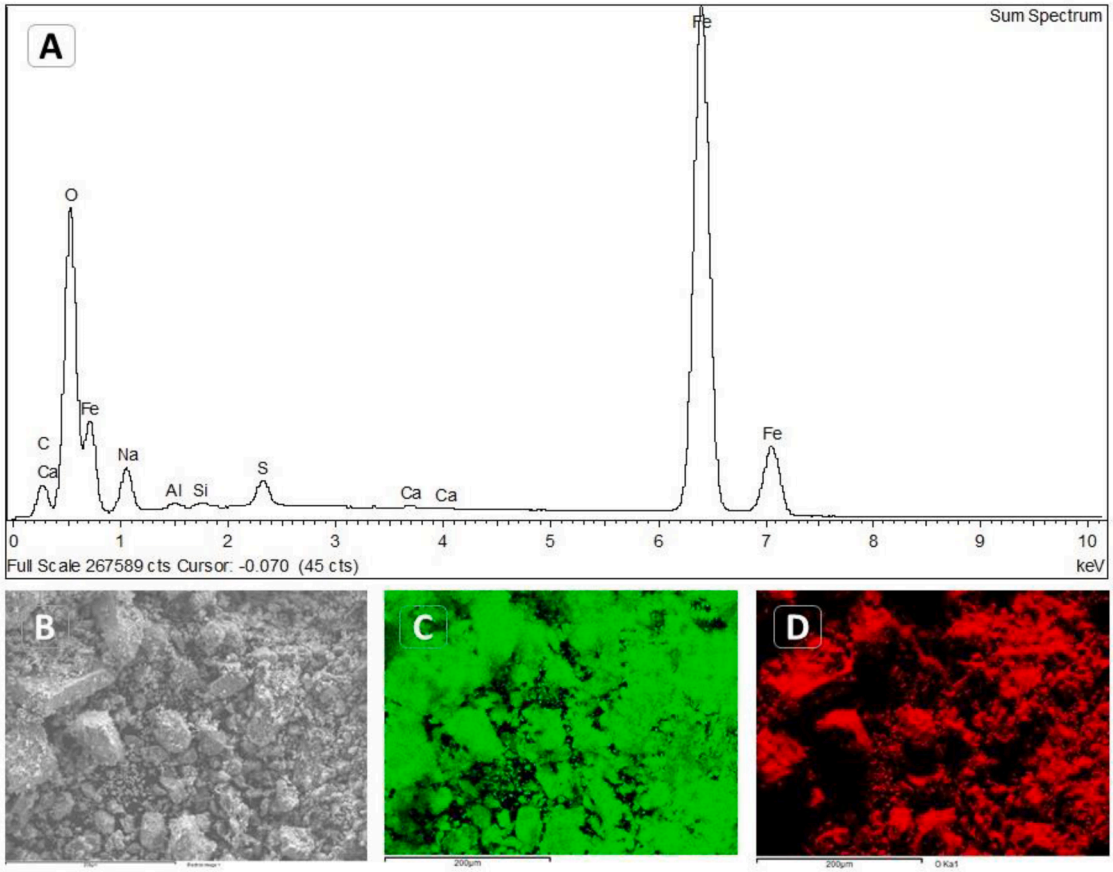

Fig. 3. MNPs observed in EDX spectrum (A), electron micrograph region at 200 μm (B), distribution of Fe in elemental mapping (C), and distribution of O in elemental mapping (D).

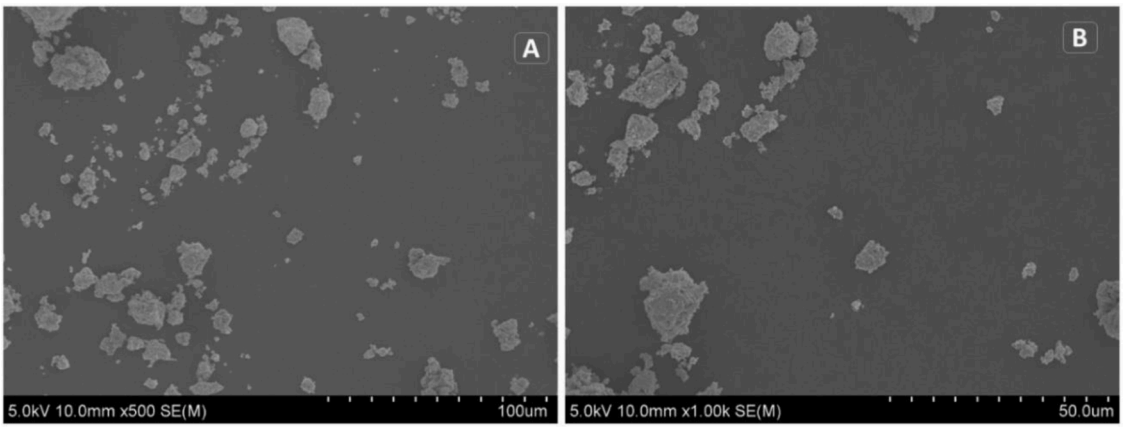

Fig. 4. SEM micrograph shows irregular flake-like clusters at magnification and scale bar of 500x and 100 um (a), and 1000x and 50 um (b), respectively. Operating conditions were accelerating voltage of 5.0 kV, and working distance of 10.0 mm.

approaches, and so the option of silanization by APTES was rejected on grounds of toxicity.

It is also worth noting that covalent immobilization may lead to changes in the native structure of the enzymes, causing serious loss of enzymatic activity [57]. Moreover, improving the covalent immobilization method would not only ultimately increase the activity recovery, but also suppress the enzyme leaching from the surface of MNPs [58].

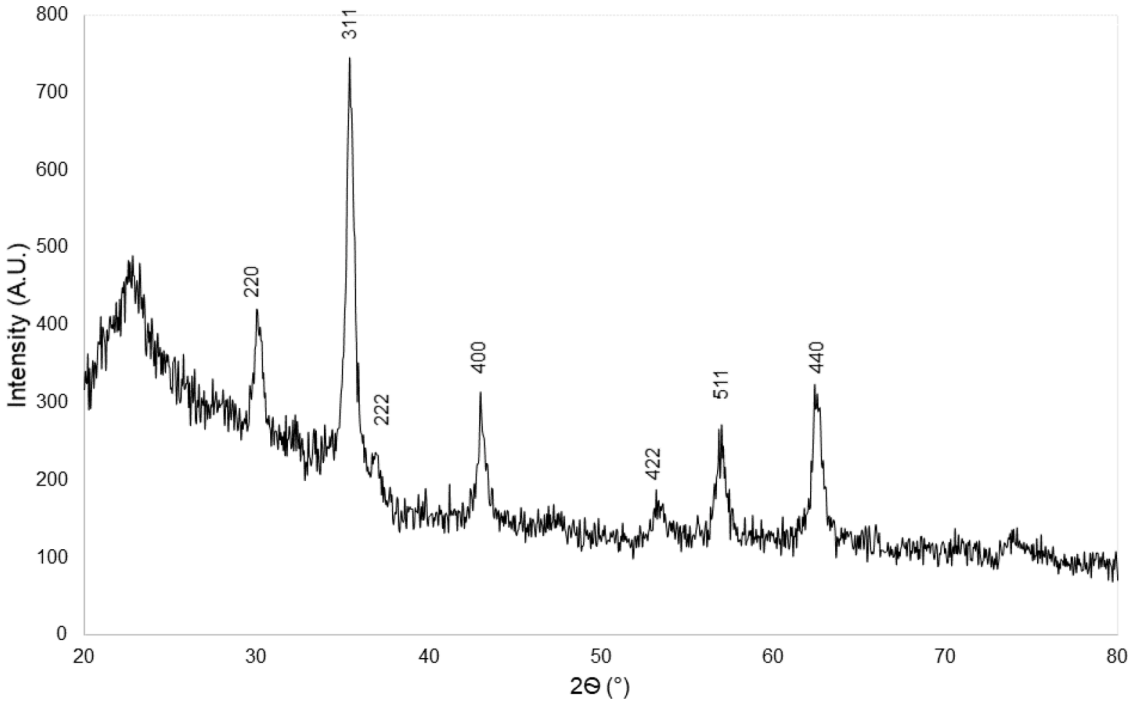

Fig. 5. X-ray powder diffraction patterns of the MNPs. Radiation source (Cu Kα1) operated at a voltage of 40 keV and current of 30 mA.

3.5. Evaluation of the nano-immobilized enzymes (MNPs@GLU-ENZ)

The effect of temperature on the activity of free and immobilized enzymes was evaluated by assaying the enzyme activity at different temperatures (20 - 80 °C) and pH 5.0. The results shown in Fig. 6a indicated that immobilization did not change the optimal temperature of pectinase and xylanase (50 °C and 60 °C, respectively). This agrees with the typical temperatures for optimum activation of commercial pectinase (50 °C) and xylanolytic thermostable enzymes (60 °C). Additionally, the immobilized pectinase and xylanase retained 80% activity over a wider temperature range of 30–80 °C and 40–80 °C, respectively, compared to the free enzymes (which retained enzyme activity more than 80% over range of 30–70 °C and 50–70 °C, respectively). The improved retention of enzyme activity of the immobilized enzymes above the optimum temperature, with no shift in the optimum temperature, might be ascribed to the covalent bonding to MNPs, which in turn prevented the conformational change of enzymes at high temperature [55].

The influence of pH on the activity of free and immobilized enzymes was studied by assaying at varying pH values ranging from 2.0 to 11.0 at 50 °C. The results shown in Fig. 6b indicated that immobilization did not change the optimal pH (5.0) of pectinase and xylanase. Moreover, the pH activity scope of the immobilized pectinase was expanded, retaining more than 80% activity over a wider pH range of 4.0–8.0, compared with that of the free form (pH range of 5.0–7.0). One possible reason for this could be the compact conformational structure of enzyme in the polymeric network of nanocarrier [15]. On the other hand, immobilized xylanase was slightly shifted toward the neutral range compared to the free form. Immobilized xylanase retained more than 80% activity in a pH range of 4.0–7.0 compared with that of the free form (pH range of 3.0–6.0). The slight shift of pH activity for immobilized xylanase might be attributed to partitioning effects of polyionic matrices [27].

Storage stability of the free and immobilized enzymes was evaluated at 5-day intervals by storing them at 6 °C for 30 days. As shown in Fig. 6c, the immobilization with magnetic nanoparticles improved the stability of enzymes. The immobilized pectinase and xylanase retained about 56% and 53% of their initial activity after 30 days and 25 days, respectively. This compares with the free pectinase and xylanase, which retained about 43% and 49% of their initial activity after 25 days and 20 days, respectively. These results suggested that the immobilization with magnetic nanoparticles might improve conservation and stabilization of the structural conformation of enzymes which preventing possible distortion effects on the active sites of enzyme [18].

From a process economics perspective, the reusability aspect of immobilized enzymes is a key consideration for industrial applicability. Thus, the useful lifetime of immobilized enzymes in the present work was assessed by subjecting the preparations to 6 successive process cycles (Fig. 6d). After one cycle was over, the immobilized enzymes were removed from the reaction medium with an external magnetic field and reused again to check durability. The residual activity of immobilized enzymes was 56% for pectinase and 52% for xylanase, after four and three consecutive cycles, respectively. The activity loss of immobilized enzyme probably could be due to enzyme denaturation due to recurrent encountering of substrate to the active site of immobilized enzyme after each successive use [59]. Previous studies have shown that the activity of hydrolytic enzymes bound to MNPs show a 20% decrease after the second re-use [23], which may be explained by such factors as enzyme detachment, the effect of temperature on reducing the magnetization of MNPs and interference by components of the reaction mixture [60]. Encapsulation of MNPs in chitosan for the dual purpose of

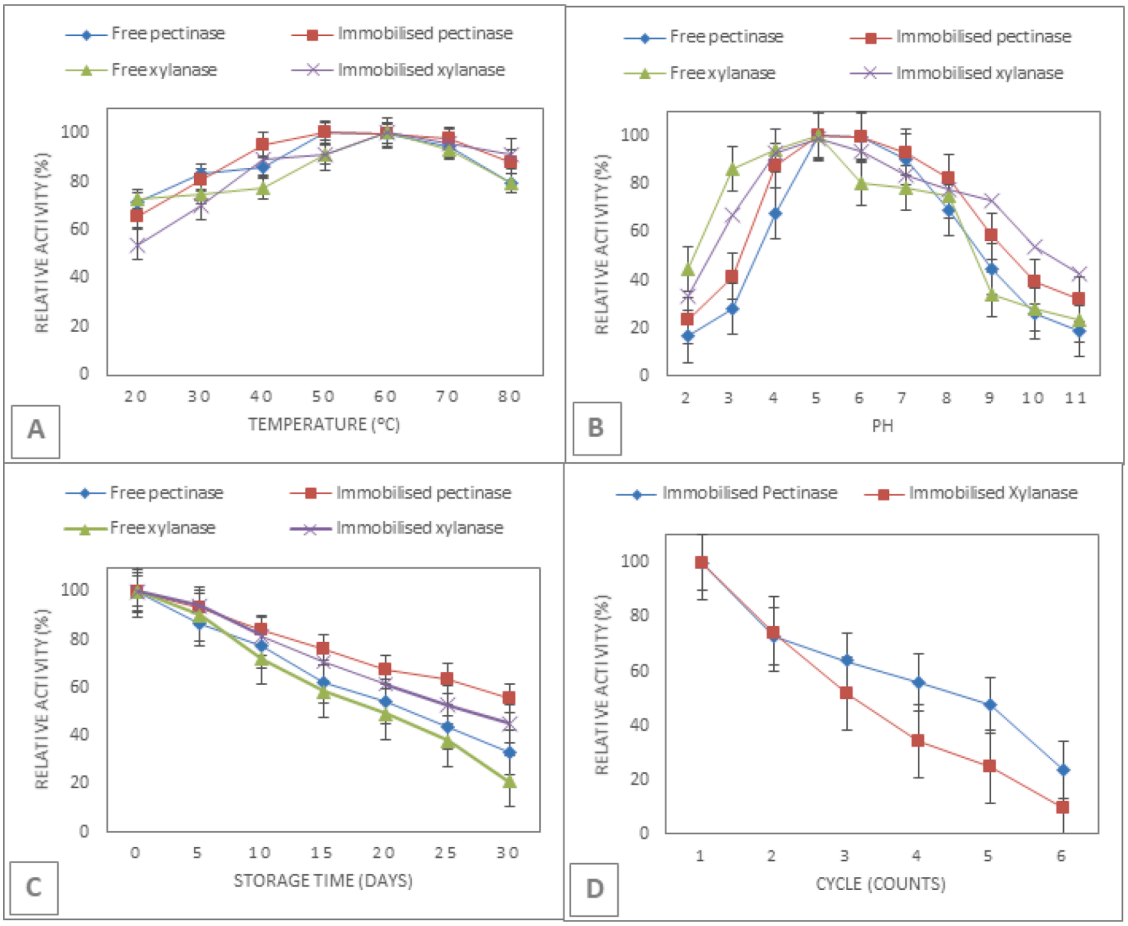

Fig. 6. Panels (A–C) shows the effect of temperature (A), pH (B), storage time (C), and recycle count (D) on relative activity of immobilized pectinase and xylanase in comparison with free enzyme. Error bars represent the standard error of the mean (n= 3). Means of treatments were significantly different ($P < 0.05$) based on one-way ANOVA.

functualization and leachate reduction have been reported [62]. In such a case, enzymes can be immobilized on the surface of chitosan and achieve the magnetic separation and recycling of the immobilized enzymes from the reaction medium.

4. Conclusions

Superparamagnetic magnetite nanoparticles were biosynthesized using *A. flavus*. The particles were found to be flake-like, with average crystallite size of ~16 nm. Pectinase and xylanase were individually immobilized on the surface of MNPs. The immobilized enzymes were more stable at wider ranges of pH and temperatures. Furthermore, reusability and storage stability of the enzymes were improved by immobilization. Such promising results may open route for potential applications in fruit juice extraction and clarification.

Author contributions

Hassan, S.S., Conceptualization; Hassan, S.S., Jaiswal, A.K., Data curation; Hassan, S.S., Formal analysis; Hassan, S.S., Williams, G. A., and Jaiswal, A.K., Funding acquisition; Hassan, S.S., Investigation; Hassan, S.S., Williams, G.A., Jaiswal, A.K., and Duffy, B., Methodology; Williams, G.A., and Jaiswal, A.K., Project administration; Williams, G.A., Jaiswal, A.K., and Duffy, B., Resources; Hassan, S.S., Jaiswal, A.K., Software; Williams, G.A., and Jaiswal, A.K., Supervision; Williams, G.A., and Jaiswal, A.K., Validation; Hassan, S.S., Visualization; Hassan, S.S., Original draft; Hassan, S.S., Williams, G.A., Jaiswal, A.K., and Duffy, B., Review & editing. All authors have read and agreed to the published version of the manuscript.

Declaration of Competing Interest

The authors declare no conflict of interest. The funding body had no role in the design of the study; in the collection, analysis, or

interpretation of data; in the writing of the manuscript; or in the decision to publish the results.

Acknowledgments

The authors gratefully acknowledge the assistance from Aoife Power with the XRD and SEM analysis.

Funding

The authors would like to acknowledge the funding from Technological University Dublin - City Campus, Dublin, Ireland under the Fiosraigh Scholarship program, 2017.

References

[1] P. Rasor, Immobilized Enzymes in Enantioselective Organic Synthesis. Chiral Catalyst Immobilization and Recycling, John Wiley & Sons, 2008, pp. 97–121. De Vos, D., Vankelecom, F.J., Jacobs, P.A.
[2] C.L.B. Reis, E.Y.A. de Sousa, J. de França Serpa, R.C. Oliveira, J.C.S. Dos Santos, Design of immobilized enzyme biocatalysts: drawbacks and opportunities, Quim. Nova 42 (2019) 768–783, https://doi.org/10.21577/0100-4042.20170381.
[3] B.C.C. Research, Nanotechnol. Adv. Mater. Res. Rev. (2019) https://www.bccresearch.com/market-research/nanotechnology/nanotechnology-fuel-cell-research-review.html (accessed June 22, 2020).
[4] M. Bilal, Y. Zhao, T. Rasheed, H.M.N. Iqbal, Magnetic nanoparticles as versatile carriers for enzymes immobilization: a review, Int. J. Biol. Macromol. 120 (2018) 2530–2544.
[5] J.W. Moon, C.J. Rawn, A.J. Rondinone, L.J. Love, Y. Roh, S.M. Everett, R.J. Lauf, T.J. Phelps, Large-scale production of magnetic nanoparticles using bacterial fermentation, J. Ind. Microbiol. Biotechnol. 37 (2010) 1023–1031, https://doi.org/10.1007/s10295-010-0749-y.
[6] M.E. Cueva, L.E. Horsfall, The contribution of microbially produced nanoparticles to sustainable development goals, Microb. Biotechnol. 10 (2017) 1212–1215, https://doi.org/10.1111/1751-7915.12788.
[7] M.L. Verma, S. Sharma, K. Dhiman, A.K. Jana, R. Prasad, Microbial Production of Nanoparticles: mechanisms and Applications, in: Microbial Nanobionics, 1, Springer, 2019, pp. 159–176.
[8] L.P. Silva, C.C. Bonatto, V.L. Polez, R. Prasad, Green Synthesis of Metal Nanoparticles by Fungi: current Trends and Challenges. Advances and Applications Through Fungal Nanobiotechnology, Springer, 2016, pp. 71–89.
[9] A. Bharde, D. Rautaray, V. Bansal, A. Ahmad, I. Sarkar, S.M. Yusuf, M. Sanyal, M. Sastry, Extracellular biosynthesis of magnetite using fungi, Small 2 (2006) 135–141, https://doi.org/10.1002/smll.200500180.
[10] S. Mahanty, M. Bakshi, S. Ghosh, S. Chatterjee, S. Bhattacharyya, P. Das, S. Das, P. Chaudhuri, Green Synthesis of Iron Oxide Nanoparticles Mediated by Filamentous Fungi Isolated from Sundarban Mangrove Ecosystem, India, Bionanoscience 9 (2019) 637–651, https://doi.org/10.1007/s12668-019-00644-w.
[11] M. Abdeen, S. Sabry, H. Ghozlan, A.A. El-Gendy, E.E. Carpenter, Microbial-Physical Synthesis of Fe and Fe_3O_4 Magnetic Nanoparticles Using *Aspergillus niger* YESM1 and Supercritical Condition of Ethanol, J. Nanomater. (2016), https://doi.org/10.1155/2016/9174891.
[12] S. Chatterjee, S. Mahanty, P. Das, P. Chaudhuri, S. Das, Biofabrication of iron oxide nanoparticles using manglicolous fungus *Aspergillus niger* BSC-1 and removal of Cr(VI) from aqueous solution, Chem. Eng. J. 385 (2020), 123790, https://doi.org/10.1016/j.cej.2019.123790.
[13] Chandra Tarafdar, J. Raliya, R. Rapid, Low-Cost, and Ecofriendly Approach for Iron Nanoparticle Synthesis Using *Aspergillus oryzae* TFR9, J. Nanoparticles 4 (2013), 141274, https://doi.org/10.1155/2013/141274.
[14] A. Bhargava, N. Jain, L., .M.. Barathi, M.S. Akhtar, Y.S. Yun, J Panwar, Synthesis, characterization and mechanistic insights of mycogenic iron oxide nanoparticles, J. Nanoparticle Res. (2013) 15, https://doi.org/10.1007/s11051-013-2031-5.
[15] S. Kharazmi, A. Taheri-Kafrani, A. Soozanipour, Efficient immobilization of pectinase on trichlorotriazine-functionalized polyethylene glycol-grafted magnetic nanoparticles: a stable and robust nanobiocatalyst for fruit juice clarification, Food Chem 325 (2020), 126890, https://doi.org/10.1016/j.foodchem.2020.126890.
[16] L. Dal Magro, K.S. de Moura, B.E. Backes, E.W. de Menezes, E.V. Benvenutti, S. Nicolodi, M.P. Klein, R. Fernandez-Lafuente, R.C. Rodrigues, Immobilization of pectinase on chitosan-magnetic particles: influence of particle preparation protocol on enzyme properties for fruit juice clarification, Biotechnol. Rep. 24 (2019) e00373, https://doi.org/10.1016/j.btre.2019.e00373.
[17] G. Fang, H. Chen, Y. Zhang, A. Chen, Immobilization of pectinase onto Fe_3O_4@SiO_2-NH_2 and its activity and stability, Int. J. Biol. Macromol. 88 (2016) 189–195, https://doi.org/10.1016/j.ijbiomac.2016.03.059.
[18] U.V. Sojitra, S.S. Nadar, V.K. Rathod, Immobilization of pectinase onto chitosan magnetic nanoparticles by macromolecular cross-linker, Carbohydr. Polym. 157 (2017) 677–685, https://doi.org/10.1016/j.carbpol.2016.10.018.
[19] L. Mosafa, M. Shahedi, M. Moghadam, Magnetite Nanoparticles Immobilized Pectinase: preparation, Characterization and Application for the Fruit Juices Clarification, J. Chinese Chem. Soc. 61 (2014) 329–336, https://doi.org/10.1002/jccs.201300347.
[20] S.S. Nadar, V.K. Rathod, A co-immobilization of pectinase and cellulase onto magnetic nanoparticles for antioxidant extraction from waste fruit peels, Biocatal. Agric. Biotechnol. (2018), https://doi.org/10.1016/j.bcab.2018.12.015.
[21] V. Singh, S. Kaul, P. Singla, V. Kumar, R. Sandhir, J.H. Chung, P. Garg, N.K. Singhal, Xylanase immobilization on magnetite and magnetite core/shell nanocomposites using two different flexible alkyl length organophosphonates: linker length and shell effect on enzyme catalytic activity, Int. J. Biol. Macromol. 115 (2018) 590–599, https://doi.org/10.1016/j.ijbiomac.2018.04.097.
[22] A. Kumar, S.K.S. Patel, B. Mardan, R. Pagolu, R. Lestari, S.H. Jeong, T. Kim, J.R. Haw, S.Y. Kim, I.W. Kim, et al., Immobilization of xylanase using a protein-inorganic hybrid system, J. Microbiol. Biotechnol. 28 (2018) 638–644, https://doi.org/10.4014/jmb.1710.10037.
[23] A. Amaro-Reyes, A. Díaz-Hernández, J. Gracida, B.E. García-Almendárez, M. Escamilla-García, T. Arredondo-Ochoa, C. Regalado, Enhanced Performance of Immobilized Xylanase/Filter Paper-ase on a Magnetic Chitosan Support, Catalysts 9 (2019) 966, https://doi.org/10.3390/catal9110966.
[24] A. Hamzah, S. Ainiyah, D. Ramadhani, G.E.K. Parwita, Y. Rahmawati, H. Soeprijanto; Ogino, A. Widjaja, Cellulase And Xylanase Immobilized on Chitosan Magnetic Particles for Application In Coconut Husk Hydrolysis, Int. J. Technol. 10 (2019) 613–623, https://doi.org/10.1017/CBO9781107415324.004.
[25] A. Landarani-Isfahani, A. Taheri-Kafrani, M. Amini, V. Mirkhani, M. Moghadam, A. Soozanipour, A. Razmjou, Xylanase Immobilized on Novel Multifunctional Hyperbranched Polyglycerol-Grafted Magnetic Nanoparticles: an Efficient and Robust Biocatalyst, Langmuir 31 (2015) 9219–9227, https://doi.org/10.1021/acs.langmuir.5b02004.
[26] V. Mehnati-Najafabadi, A. Taheri-Kafrani, A.K. Bordbar, A. Eidi, Covalent immobilization of xylanase from *Thermomyces lanuginosus* on aminated superparamagnetic graphene oxide nanocomposite, J. Iran. Chem. Soc. 16 (2019) 21–31, https://doi.org/10.1007/s13738-018-1477-x.
[27] M.Q. Liu, X.J. Dai, R.F. Guan, X. Xu, Immobilization of *Aspergillus niger* xylanase A on Fe_3O_4-coated chitosan magnetic nanoparticles for xylooligosaccharide preparation, Catal. Commun. 55 (2014) 6–10, https://doi.org/10.1016/j.catcom.2014.06.002.
[28] A. Kumari, P. Kaila, P. Tiwari, V. Singh, S. Kaul, N. Singhal, P. Guptasarma, Multiple thermostable enzyme hydrolases on magnetic nanoparticles: an immobilized enzyme-mediated approach to saccharification through simultaneous xylanase, cellulase and amylolytic glucanotransferase action, Int. J. Biol. Macromol. 120 (2018) 1650–1658, https://doi.org/10.1016/j.ijbiomac.2018.09.106.
[29] S. Kumar, I. Haq, A. Yadav, J. Prakash, A. Raj, Immobilization and Biochemical Properties of Purified Xylanase from *Bacillus amyloliquefaciens* SK-3 and Its Application in Kraft Pulp Biobleaching, J. Clin. Microbiol. Biochem. Technol. (2016) 026–034, https://doi.org/10.17352/jcmbt.000012.

[30] S.S. Hassan, B.K. Tiwari, G.A. Williams, A.K. Jaiswal, Bioprocessing of brewers ' spent grain for production of xylanopectinolytic enzymes by *Mucor sp*, Bioresour. Technol. Rep. 9 (2020), 100371, https://doi.org/10.1016/j.biteb.2019.100371.

[31] G.L. Miller, Use of Dinitrosalicylic Acid Reagent for Determination of Reducing Sugar, Anal. Chem. 31 (1959) 426–428, https://doi.org/10.1021/ac60147a030.

[32] H. Nait M'barek, B. Taidi, T. Smaoui, M. Aziz, A. Ben; Mansouri, H. Hajjaj, Nait M'barek; Isolation, screening and identification of ligno-cellulolytic fungi from northern central Morocco, Biotechnol. Agron. Soc. Environ. 23 (2019) 207–217, https://doi.org/10.25518/1780-4507.18182ï.

[33] P. Scherrer, Determination of the size and the internal structure of colloidal particles by means of X-rays, News from *Soc. Sci.* Göttingen 2 (1918) 98–100.

[34] A. Ghadi, F. Tabandeh, S. Mahjoub, A. Mohsenifar, F. Talebnia Roshan, Shafiee Alavije, R. Fabrication and Characterization of Core-Shell Magnetic Chitosan Nanoparticles as a Novel carrier for Immobilization of Burkholderia cepacia Lipase, J. Oleo. Sci. 64 (2015) 423–430, https://doi.org/10.5650/jos.ess14236.

[35] P. Kaur, M.S. Taggar, A. Kalia, Characterization of magnetic nanoparticle–immobilized cellulases for enzymatic saccharification of rice straw, Biomass Convers. Biorefinery (2020) 1–15, https://doi.org/10.1007/s13399-020-00628-x.

[36] M.M. Bradford, A rapid and sensitive method for the quantitation of microgram quantities of protein utilizing the principle of protein-dye binding, Anal. Biochem. 72 (1976) 248–254, https://doi.org/10.1016/0003-2697(76)90527-3.

[37] Y. Zhou, S. Pan, X. Wei, L. Wang, Y. Liu, Immobilization of β-glucosidase onto magnetic nanoparticles and evaluation of the enzymatic properties, Bioresources 8 (2013) 2605–2619, https://doi.org/10.15376/biores.8.2.2605-2619.

[38] G.L. Miller, Use of Dinitrosalicylic Acid Reagent for Determination of Reducing Sugar, Anal. Chem. 31 (1959) 426–428, https://doi.org/10.1021/ac60147a030.

[39] A. Xiao, C. Xu, Y. Lin, H. Ni, Y. Zhu, H. Cai, Preparation and characterization of κ-carrageenase immobilized onto magnetic iron oxide nanoparticles, Electron. J. Biotechnol. 19 (2016) 1–7, https://doi.org/10.1016/j.ejbt.2015.10.001.

[40] Saleem, A.R. Mycobiota and molecular detection of *Aspergillus flavus* and *A. parasiticus* aflatoxin contamination of Strawberry (*Fragaria ananassa* Duch.) fruits. *Arch. Phytopathol. Plant Prot.* 2017, 50, 982–996, doi:10.1080/03235408.2017.1411155.

[41] S.K. Dorcheh, K. Vahabi, Biosynthesis of Nanoparticles by Fungi: large-Scale Production. Fungal Metabolites, Springer International Publishing, 2016, pp. 1–20.

[42] S. Saranya, K. Vijayarani, S. Pavithra, Green Synthesis of Iron Nanoparticles using Aqueous Extract of *Musa ornata* Flower Sheath against Pathogenic Bacteria, Indian J. Pharm. Sci. 79 (2017) 688–694, https://doi.org/10.4172/pharmaceutical-sciences.1000280.

[43] S.S.U. Rahman, M.T. Qureshi, K. Sultana, W. Rehman, M.Y. Khan, M.H. Asif, M. Farooq, N. Sultana, Single step growth of iron oxide nanoparticles and their use as glucose biosensor, Res. Phys. 7 (2017) 4451–4456, https://doi.org/10.1016/j.rinp.2017.11.001.

[44] N.S. Kavitha, K.S. Venkatesh, N.S. Palani, R. Ilangovan, Fungus mediated biosynthesis of WO_3 nanoparticles using *Fusarium solani* extract, in: Proceedings of the AIP Conference Proceedings 1832, American Institute of Physics Inc., 2017, 050130.

[45] E.A. Campos, D.V.B.S. Pinto, J.I.S. de Oliveira, E. Mattos, C. da, R. Dutra, C.L. de, Synthesis, characterization and applications of iron oxide nanoparticles - A short review, J. Aerosp. Technol. Manag. 7 (2015) 267–276.

[46] N. Huang, Y. Xu, D. Jiang, High-performance heterogeneous catalysis with surface-exposed stable metal nanoparticles, Sci. Rep. 4 (2014) 1–8, https://doi.org/10.1038/srep07228.

[47] H. Fatima, D.W. Lee, H.J. Yun, K.S. Kim, Shape-controlled synthesis of magnetic Fe_3O_4 nanoparticles with different iron precursors and capping agents, RSC Adv. 8 (2018) 22917–22923, https://doi.org/10.1039/c8ra02909a.

[48] Y.P. Yew, K. Shameli, M. Miyake, N.B. Bt Ahmad Khairudin, S.E. Bt Mohamad, H. Hara, M.F. Bt Mad Nordin, K.X. Lee, An eco-friendly means of biosynthesis of superparamagnetic magnetite nanoparticles via marine polymer, IEEE Trans. Nanotechnol. 16 (2017) 1047–1052, https://doi.org/10.1109/TNANO.2017.2747088.

[49] K.S. Loh, Y.H. Lee, A. Musa, A.A. Salmah, I. Zamri, Use of Fe3O4 nanoparticles for enhancement of biosensor response to the herbicide 2,4-dichlorophenoxyacetic acid, Sensors 8 (2008) 5775–5791, https://doi.org/10.3390/s8095775.

[50] A. Bhargava, N. Jain, L.M. Barathi, M.S. Akhtar, Y.S. Yun, J. Panwar, Synthesis, characterization and mechanistic insights of mycogenic iron oxide nanoparticles. Nanotechnology For Sustainable Development, 1st Edition, Springer International Publishing, 2014, pp. 337–348. ISBN 9783319050416.

[51] J. Namanga, J. Foba, D.T. Ndinteh, D.M. Yufanyi, R. Werner, M. Krause, Synthesis and Magnetic Properties of a Superparamagnetic Nanocomposite '"Pectin-Magnetite Nanocomposite, J. Nanomater. (2013), https://doi.org/10.1155/2013/137275.

[52] J. Xu, J. Sun, Y. Wang, J. Sheng, F. Wang, M. Sun, Application of iron magnetic nanoparticles in protein immobilization, Molecules 19 (2014) 11465–11486, https://doi.org/10.3390/molecules190811465.

[53] C. Masi, C. Chandramohan, M.F. Ahmed, Immobilization of the Magnetic Nanoparticles with Alkaline Protease Enzyme Produced by *Enterococcus hirae* and *Pseudomonas aeruginosa* Isolated from Dairy Effluents, Brazilian Arch. Biol. Technol. (2018) 60, https://doi.org/10.1590/1678-4324-2017160572.

[54] V.M. Costa, M.C.M. De Souza, P.B.A. Fechine, A.C. Macedo, L.R.B. Gonçalves, Nanobiocatalytic systems based on lipase-Fe3O4 and conventional systems for isoniazid synthesis: a comparative study, Brazilian J. Chem. Eng. 33 (2016) 661–673, https://doi.org/10.1590/0104-6632.20160333s20150137.

[55] A.B. Muley, A.S. Thorat, R.S. Singhal, K. Harinath Babu, A tri-enzyme co-immobilized magnetic complex: process details, kinetics, thermodynamics and applications, Int. J. Biol. Macromol. 118 (2018) 1781–1795, https://doi.org/10.1016/j.ijbiomac.2018.07.022.

[56] M. Perwez, R. Ahmad, M. Sardar, A reusable multipurpose magnetic nanobiocatalyst for industrial applications, Int. J. Biol. Macromol. 103 (2017) 16–24, https://doi.org/10.1016/j.ijbiomac.2017.05.029.

[57] Y. Cen, Y. Liu, Y. Xue, Y. Zheng, Immobilization of Enzymes in/on Membranes and their Applications, Adv. Synth. Catal. 361 (2019) 5500–5515, https://doi.org/10.1002/adsc.201900439.

[58] F.B.H. Rehm, S. Chen, B.H.A. Rehm, Enzyme engineering for in situ immobilization, Molecules (2016) 21.

[59] A. Sahu, P.S. Badhe, R. Adivarekar, M.R. Ladole, A.B. Pandit, Synthesis of glycinamides using protease immobilized magnetic nanoparticles, Biotechnol. Rep. 12 (2016) 13–25, https://doi.org/10.1016/j.btre.2016.07.002.

[60] S. Mahanty, M. Bakshi, S. Ghosh, T. Gaine, S. Chatterjee, S. Bhattacharyya, S. Das, P. Das, P. Chaudhuri, Mycosynthesis of iron oxide nanoparticles using manglicolous fungi isolated from Indian sundarbans and its application for the treatment of chromium containing solution: synthesis, adsorption isotherm, kinetics and thermodynamics study, Environ. Nanotechnology, Monit. Manag. 12 (2019), 100276, https://doi.org/10.1016/j.enmm.2019.100276.

[61] Y.S. Chung, M.Y. Jeon, C.K. Kim, Fabrication of Nearly Monodispersed Silica Nanoparticles by Using Poly(1-vinyl-2-pyrrolidinone) and Their Application to the Preparation of Nanocomposites, Macromol. Res. 17 (2009) 37–43.

[62] T. Parandhaman, N. Pentela, B. Ramalingam, D. Samanta, S.K. Das, Metal Nanoparticle Loaded Magnetic-Chitosan Microsphere: water Dispersible and Easily Separable Hybrid Metal Nano-biomaterial for Catalytic Applications, ACS Sustain. Chem. Eng. 5 (2017) 489–501, https://doi.org/10.1021/acssuschemeng.6b01862.